

Article

Expanded Clay Production Waste as Supplementary Cementitious Material

Rimvydas Kaminskas * and Brigita Savickaite

Department of Silicate Technology, Faculty of Chemical Technology, Kaunas University of Technology, Radvilenu 19, LT-50254 Kaunas, Lithuania; brigita.savickaite@ktu.edu

* Correspondence: rimvydas.kaminskas@ktu.lt; Tel.: +370-62023774

Abstract: Global warming stands as one of the most significant challenges facing our planet, primarily due to the substantial emissions of greenhouse gases into the atmosphere. Among the major contributors to these emissions is the cement industry, which ranks as one of the largest sources of CO₂ pollutants. To address this issue, a potential solution involves partially substituting cement with alternative materials, particularly waste generated by other industries. The aim of this study was to investigate the opportunity of using an industrial waste which originates from the cleaning of flue gas in the production of expanded clay as a supplementary cementitious material. The influence of expanded clay kiln dust on the properties of Portland cement was estimated by XRD, thermal, calorimetry and compressive strength analysis. The expanded clay kiln dust was used as received and it was additionally thermally activated at 600 °C. It was determined that the original dust can be distinguished by average pozzolanic activity; meanwhile, the pozzolanic activity of additionally activated waste increased by one third. Portland cement was replaced with both types of waste in various proportions. It was found that the additive of the investigated waste accelerates the primary hydration of Portland cement, generates the pozzolanic reaction, and incites the formation of calcium silicate hydrates and hydrates containing aluminum compounds. The addition of up to 25 wt.% of activated expanded clay kiln dust leads to a higher compressive strength of samples of Portland cement.

Keywords: Portland cement; waste; supplementary cementitious materials



check for updates

Citation: Kaminskas, R.; Savickaite, B. Expanded Clay Production Waste as Supplementary Cementitious Material. *Sustainability* **2023**, *15*, 11850. <https://doi.org/10.3390/su151511850>

Academic Editor: Patrick Tang

Received: 10 July 2023

Revised: 24 July 2023

Accepted: 31 July 2023

Published: 1 August 2023



Copyright: © 2023 by the authors. Licensee MDPI, Basel, Switzerland. This article is an open access article distributed under the terms and conditions of the Creative Commons Attribution (CC BY) license (<https://creativecommons.org/licenses/by/4.0/>).

1. Introduction

The cement production process is one of the main sources of CO₂ emissions from industrial activities. The production of 1 tone of Portland cement releases 0.75–0.95 tons of CO₂. One of the main strategies aiming to reduce CO₂ emissions is to reduce the amount of cement clinker in cement. This strategy proposes substituting a part of Portland cement with supplementary cementitious materials (SCMs) [1]. SCMs can be natural or artificial, and they also can chemically react with Portland cement hydrates or be inert [2]. A particularly high CO₂ emissions reduction and energy-saving effect is achieved when SCMs originating from industrial waste are used. Of the waste currently used in the cement industry, blast furnace slag and fly ash are the most commonly consumed options because they are formed in the largest amount worldwide [3]. Other SCMs which improve the properties of cement, such as silica fume [4], rice husk ash [5] and the spent fluid catalytic cracking catalyst [6], are also widely used, but their quantities are significantly smaller. On the other hand, wastes suitable for the cement industry could be mixed with each other or with natural raw materials and, thus, increase the total share of cement clinker that can be replaced [7–9]. Therefore, it is currently important to find new potential sources of SCMs and to study their properties.

Expanded clay production waste could be one of the more viable options. If we consider the worldwide scale, expanded clay is manufactured in very large quantities [10].

Lightweight expanded clay is a lightweight substance obtainable by heating clay in a rotary kiln. For the production of expanded clay, easily fusible and bloating clay is used [11]. Most commonly, it is clay containing illite, montmorillonite, muscovite, kaolinite, as well as impurities of quartz, carbonates and other minerals [12].

The main waste of expanded clay production is dust, which is generated during the burning process. Dust originates from the cleaning of flue gas and is captured in air pollution control systems. This dust consists of a mixture of raw materials, burnt materials and fully molten particles. Due to the composition of waste, it is not returned to the production cycle because it has a negative impact on the expansion quality of the raw material. Only a small part of dust is transported to the crushing technology of the raw materials, where it is mixed with raw clay for the intensification of the crushing process.

Reclamation of the expanded clay production dust is a major problem. In the common plants of expanded clay, annually, between 20 and 25 thousand tons of dust may be formed, which is not in demand and which is, thus, subsequently stored at landfills [13]. Several ways of using this waste have been proposed. The dust originating from expanded clay production could be used in paint manufacturing [13] or else for the production of heat-resistant concretes [14].

As expanded clay production waste partially consists from burnt clay particles, there is a possibility that this waste could be used as SCMs.

Calcined clay is the most promising SCM, as clay resources are available in extremely high amounts worldwide and are second only to limestone. Calcined clay is denoted by a wide range of applications and comes at a low cost because it is fired at medium temperatures (600–900 °C). The firing of clays breaks down the crystalline structure of the clay minerals and transforms them into an amorphous and highly reactive structure. Clay minerals are divided into four main groups: kaolinite, montmorillonite/smectite, illite and chlorite, the amount of which in clay depends on the geographical location and the bedrock [15]. Kaolinite, illite and montmorillonite are aluminosilicate minerals with a layered structure consisting of repeating tetrahedral (T) and octahedral (O) layers.

Kaolinitic clays are best suited for the production of artificial SCMs because kaolinite, which is the main mineral of these clays, decomposes at the lowest temperature of all clay minerals and gives the burnt product the highest pozzolanic activity [16]. The pozzolanic activity of fired clay is due to the transformation of kaolinite to metakaolinite during heat treatment. This process transforms the crystalline structure of clay minerals into a complex amorphous structure, which retains a certain layer order. The transformation removes structural water and leaves an amorphous aluminosilicate with high internal porosity, which leads to the high pozzolanic activity. The decomposition temperature of kaolinite depends on the order in which the structural layers are arranged. Kaolinite with a disordered structure decomposes at 530–570 °C, whereas kaolinite with an ordered structure decomposes at 570–630 °C. Metakaolinite is typically composed of 50–55 wt.% SiO₂ and 40–45 wt.% Al₂O₃. Compared to further clay minerals, kaolinite features a large temperature interval between decomposition and recrystallization, which is definitely favorable for the formation of metakaolinite [17]. Since the Al-OH groups in kaolinite are arranged in octahedral interlayers, structural changes occur more readily when kaolinite is heated in comparison to other clay minerals.

Montmorillonites/smectites are a group of T-O-T clay minerals with exchangeable cations and a high capacity for interlayer water absorption and swelling. The course of dehydration and dehydroxylation of this clay mineral group is influenced by the isomorphic exchange in the tetrahedral and octahedral layers and the type of interlayer cations. Montmorillonite dehydrates at ~300 °C, and the dehydroxylation temperature depends on the sort and arrangement of the cations in the octahedral layer. Dehydroxylation usually occurs at around 700 °C. Depending on the oxide and mineral composition of the clay, the recrystallization of montmorillonite starts at temperatures above 850 °C [18]. The optimal calcining temperature for montmorillonite clays is between 800 °C and 830 °C, with a duration of 1 to 5 h. Compared to kaolinite, the activation temperature of montmorillonite

is prominently higher, and the interval between dehydroxylation and crystallization of the new phases is narrower, as the recrystallization temperature of 850 °C is reached very quickly. This makes the thermal activation of montmorillonite considerably more difficult, but montmorillonite is a good pozzolanic material when properly activated [2].

Other clay minerals achieve less pozzolanic activity during thermal treatment. Dehydroxylation of illite, a T-O-T clay mineral, occurs at a relatively low temperature (580 °C), but, during dehydroxylation of the crystalline illite, the structure is not broken down; therefore, no amorphous compounds are formed before recrystallization into spinel and corundum. Burnt illite has a much lower pozzolanic activity than kaolinite or montmorillonite [2].

Thus, it can be assumed that dust, which is generated during the burning process of expanded clay, may offer properties suitable for the production of SCMs. Investigating the properties of new materials or waste offers the opportunity to expand the range of raw materials that can be used to partially substitute cement in its various applications. This is of great significance within the cement industry, as the use of such materials not only helps decrease environmental pollution, but also promotes sustainability in the sector. Numerous manufacturers are striving to lower the clinker-to-cement ratio by incorporating less emissions-intensive materials as a replacement for clinker. Through gradual adjustments and some innovative approaches, they have been able to enhance their sustainability efforts. Therefore, this study addresses the need to assess the possibility of using expanded clay production dust as SCMs.

2. Materials and Methods

2.1. Materials

In this work, dust captured in the e-filter originating from the cleaning of flue gas during the production of expanded clay (ECD) and Portland cement CEM I 42.5 R were used. The chemical composition of the dust and Portland cement is given in Table 1.

Table 1. Chemical composition of raw materials.

Component (wt.%)	ECD	Portland Cement (OPC)
SiO ₂	44.9	19.52
Al ₂ O ₃	25.3	5.03
Fe ₂ O ₃	9.79	3.05
CaO	4.83	61.39
MgO	1.33	3.93
K ₂ O	1.46	1.06
Na ₂ O	0.27	0.12
SO ₃	0.67	2.5
P ₂ O ₅	0.35	not estimated
TiO ₂	1.06	not estimated
Other	0.10	3.4
Loss on ignition	9.84	-
Specific surface area (m ² /kg)	360	350

From the XRD analysis data (Figure 1a), ECD was estimated to contain muscovite (PDF 00-058-2037), quartz (PDF 04-008-7651), kaolinite (PDF 00-058-2005), illite (PDF 00-058-2015), calcite (PDF 04-008-0198), anorthite (PDF 04-015-1492), anatase (PDF 00-004-0477), olivine (PDF 00-003-0195) and magnesite (PDF 00-002-0871). In the XRD curve, also, a broad hump at 20–30 2θ, characteristic to the amorphous compounds, was observed.

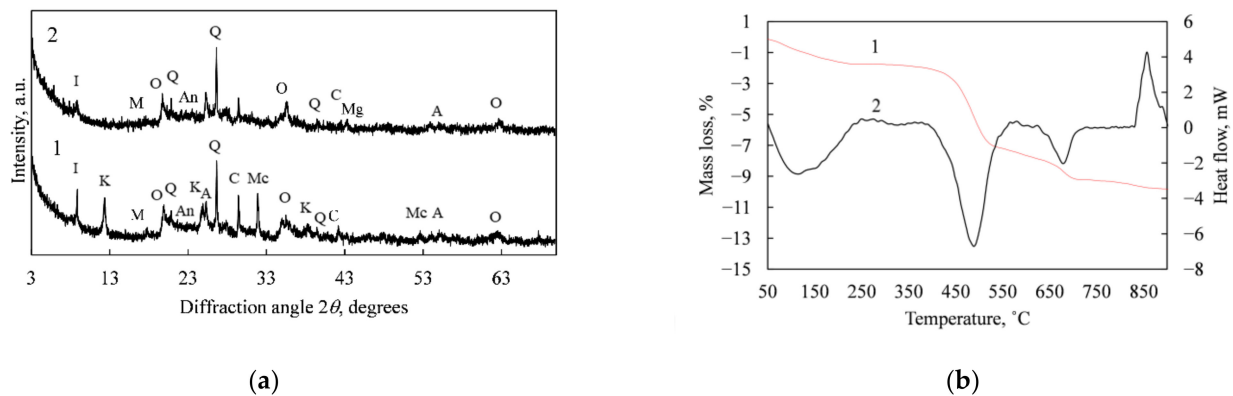


Figure 1. (a) X-ray diffraction patterns of expanded clay kiln dust as received (1) and reactivated (2), Indexes: M, muscovite $KAl_2(AlSi_3O_{10})(F,OH)_2$; Q, quartz (SiO_2); An, anorthite ($Ca(Al_2Si_2O_8)$); C, calcite ($CaCO_3$); K, kaolinite ($Al_2Si_2O_5(OH)_4$); I, illite ($K_{0.65}Al_{2.0}[Al_{0.65}Si_{3.35}O_{10}](OH)_2$); Mc, magnesite ($MgCO_3$); O, olivine ($MgFeSiO_4$); A, anatase (TiO_2); Mg, magnesium oxide (MgO). (b) Simultaneous thermal analysis (1—TG, 2—DSC) results of ECD.

In the DSC curve of ECD (Figure 1b), the endo peak at 113 °C is related with the removal of residue of water, the peak at 490 °C occurred due to the dehydroxylation of kaolinite [19], and the peak at 680 °C shows the decomposition of calcite. The exothermic peak at 857 °C indicates the formation of calcium silicates (mainly wollastonite) [20]. Thermogravimetric analysis (TGA) highlighted the total weight loss of 9.84 wt.%.

Since dust is collected in e-filters, it is quite fine and 90% of the ECD fraction was less than 48.71 μm in diameter (Figure 2). The fineness of the material is well suited for its application as supplementary cementitious materials (SCMs) without the need for additional crushing or other processing.

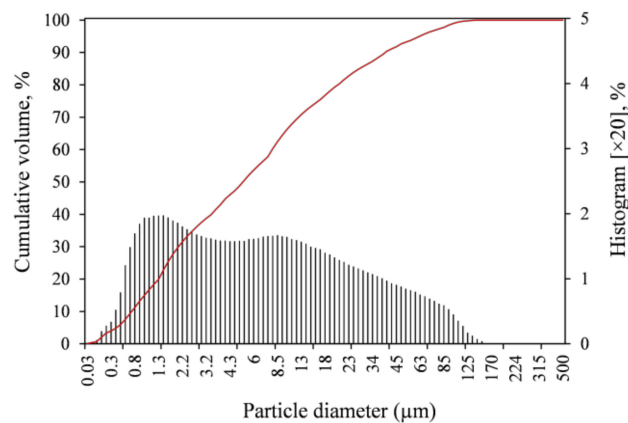


Figure 2. Particle size distribution of ECD.

2.2. Sample Preparations

Thermal reactivation of the waste. During the thermal reactivation of expanded clay production waste, it was decided to carry out this process in the laboratory, which recreates conditions analogous to the actual process of production. The ECD dust was mixed with water at a ratio of 1:0.25 to form granules of about 1 cm in diameter. The obtained pellets were dried at 90 °C for 6 h and calcined at 600 °C for 1 h. The rate of the temperature increase was 10 °C/min. The calcined granules were crushed and ground in a vibratory disc mill until a specific surface area similar to unburned waste ($360 m^2/kg$) had been achieved.

2.3. Testing Methods

Properties of cement paste were ascertained according to EN 196-3 [21].

Sand-free OPC paste was formed for instrumental analysis. After forming, the samples were kept in still water at 20 ± 1 °C for 7, 28 and 90 days. After completing the period, the specimens were comminuted and laved with isopropanol. The obtained material was desiccated at 45 °C for 12 h and stowed in hermetic bags.

Samples (prisms $40 \times 40 \times 160$ mm) for compressive strength analysis were formed according to EN 196-1 [22]. Cement–sand ratio in the samples was 1:3 and water–cement ratio 0.5:1.

Calorimetric analysis was carried out by using a TAM Air III calorimeter. The measurement deviation was <0.03 W/g. The obtained results were recalculated per gram of Portland cement.

The pozzolanic activity of ECD was determined according to NF P18-513 Standard [23]. Based on this standard, the pozzolanic activity of materials was estimated by measuring the fixed quantity of calcium hydroxide by pozzolanic materials. The amount of bound $\text{Ca}(\text{OH})_2$ was determined after 16 h of reaction between the pozzolanic additive and $\text{Ca}(\text{OH})_2$ at a temperature of 85 ± 5 °C. Titration was carried out by using 0.1 N HCl solution and 0.1% phenolphthalein dissolved in 50% alcohol as the indicator. The amount of $\text{Ca}(\text{OH})_2$ bound with the pozzolanic additive, in mg, was calculated by the formula:

$$\text{Amount of bounded } \text{Ca}(\text{OH})_2, \text{ mg/g pozzolana} = 2 \frac{V_1 - V_2}{V_1} \frac{74}{56} \times 1000;$$

where V_1 is the amount of titrated 0.1 N HCl for the blank sample and V_2 is the amount of titrated 0.1 N HCl for the sample with the additive.

The specific surface area was determined using an automatic Blaine apparatus manufactured by TESTING Bluhm & Feuerherdt GmbH.

XRD data was collected by using the D8 Advance diffractometer. Specimens were scanned in the 2θ angle range of $3\text{--}70^\circ$ with a step of 0.02° .

XRD analysis was appended by Rietveld development. For this analysis, 10 wt.% ZnO was used as an internal standard to determine the amount of amorphous compounds. The analysis was implemented by using Topas 4.1 software.

XRF was fulfilled on a Bruker X-ray S8 Tiger WD spectrometer by using SPECTRAPLUS V.2 QUANT EXPRESS software.

The thermal analysis was fulfilled by using a Netzsch STA 409 PC Luxx analyzer with ceramic sample handlers and Pt-Rh crucibles. The heating rate was 10 °C/min up to 1000 °C (± 3 °C) in a nitrogen atmosphere under environment pressure. The mass loss of specimens was assessed by the tangential method.

The mass proportion of calcium hydroxide (M_{CH}) in hardened cement paste was evaluated via equation $M_{\text{CH}} = 74/18 M_{\text{P}} + 74/44 M_{\text{C}}$, where M_{P} and M_{C} are the mass alteration caused by the decomposition of portlandite and calcite, respectively [24,25].

3. Results and Discussion

3.1. Thermal Reactivation of the Waste

Based on the results of XRD and thermal analysis, it can be stated that ECD contains a considerable amount of undehydroxylated kaolinite. Consequently, a decision was made to reheat the tested waste at a temperature of 600 °C, aligned with the point where the kaolinite dehydroxylation ends (as shown in Figure 1b). This temperature choice also corresponds to the findings of other studies [17].

After thermal reactivation of the waste, the quantity of amorphous phase by XRD/Rietveld analysis and pozzolanic activity of both materials (as received (ECD) and reactivated (RECD)) were determined (Figure 3).

The pozzolanic activity of ECD (626 mg CaO/g) corresponded to the average pozzolanic activity value; meanwhile, the activity of additional thermally activated waste increased by a third and reached 965 mg CaO/g. It should be noted that this value is only slightly lower than the activity of pure metakaolinite determined by analogous method (1068 mg CaO/g) [26].

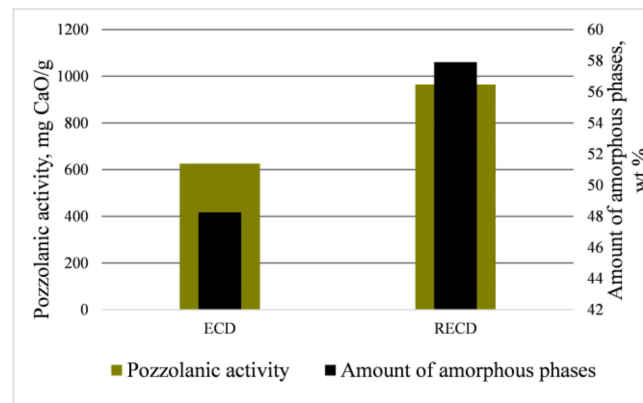


Figure 3. Amount of amorphous phase and pozzolanic activity of ECD and RECD.

The amount of amorphous phases is higher for RECD (57.9 wt.%) than for ECD (48.25 wt.%). It should also be noted that additional combustion at 600 °C does not change the composition of the waste, except for the fact that only rests of kaolinite and magnesite remain in the activated waste.

3.2. The Influence of the Waste on Cement Paste Properties

Since RECD is denoted by significantly better pozzolanic properties, activated waste was chosen to determine the influence of the expanded clay production waste on cement hydration and hardening. This waste was used to replace 10–30% of Portland cement by weight, but, to compare the results, tests were also carried out with 20 wt.% ECD additive.

The influence of the additives on cement paste properties was determined. The obtained results are presented in Table 2.

Table 2. The water-to-cement (W/C) ratio and setting time of Portland cement paste.

Sample	W/C	Setting Time (min)	
		Initial	Final
OPC	0.273	100	145
OPC + 10 wt.% RECD	0.313	130	190
OPC + 20 wt.% RECD	0.345	235	285
OPC + 25 wt.% RECD	0.362	290	340
OPC + 30 wt.% RECD	0.38	320	378
OPC + 20 wt.% ECD	0.329	170	230

As can be seen from the presented data, the investigated additives increase the water demand of cement and prolong the setting time. This can be explained by the fact that, due to the wetting effect of clay particles, calcined clay usually increases water demand [27]. The retardation in the setting times is due to the presence of incompletely burned clay particles and the effect of a lower cement content [28]. On the other hand, ECD requires less water for cement paste compared to RECD, and the setting time with ECD additive is also shorter.

3.3. The Influence of the Waste on Portland Cement Hydration and Hardening

The outcome of the calorimetric analysis is presented in Figure 4. In the samples with additives, the induction period lasted about 1 h longer than in the samples of Portland cement (Figure 4a). Another peak of heat emission, pertaining to the hydration of calcium silicates, is upwards intensive in the specimen without additives. Yet, in samples with ECD additive, the intensity of this peak is only slightly smaller. Meanwhile, in the samples with RECD additives, the intensity of this peak directly depends on the amount of the additive, i.e., the higher the amount of the additive, the more intense the peak.

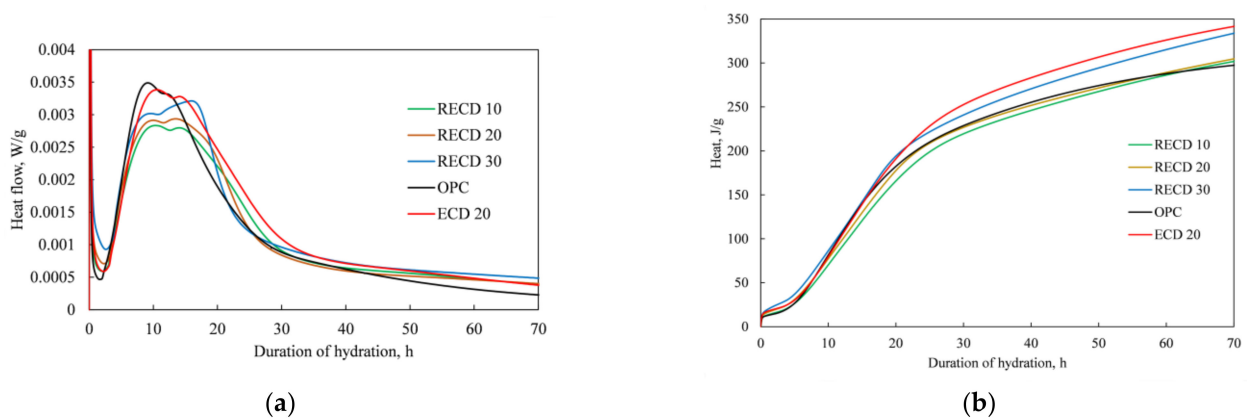


Figure 4. The calorimetric analysis results of samples: (a) heat flow; (b) total heat.

An essential disparity in the heat flow graphs is observable in the zone of the aluminate phase hydration reaction, which is defined by the hump in the second peak. This hump in the samples with both additives is more clearly noticeable, whereas, in the samples with 20 wt.% and 30 wt.% RECD additive, this shoulder is more intensive compared to the second heat emission peak.

More heat of hydration (304–343 J/g) was determined (Figure 4b) in all samples with SCMs than in the sample of blank Portland cement (298 J/g) up to 70 h of hydration.

To summarize the results of heat evolution, it can be stated that both additives—the thermally activated one and the nonactivated one—have been found to accelerate the primary hydration of cement, especially the hydration reactions of the aluminate-bearing phase.

XRD analysis of the specimens hydrated for 28 days is presented in Figure 5. XRD data indicated that, in all samples, regular cement hydrates—ettringite (PDF 41-1451) and portlandite ($\text{Ca}(\text{OH})_2$) (PDF 84-1271)—are formed. Also, non-hydrated calcium silicates (C_3S , C_2S) (PDF 42-551) were identified in the samples. In addition to these compounds, the XRD curves show peaks for the calcite (CaCO_3) (PDF 5-586) and periclase (MgO) (PDF 00-001-1235). It should be noted that, in the samples with additives, XRD analysis does not identify any new compounds containing aluminum-bearing phases. This may be related to the formation of amorphous or semi-crystalline aluminum-containing hydrates in the hardening cement. An essential difference is observed for intensities of the portlandite and unhydrated calcium silicates peaks: the curves of the samples with the additives are characterized by lower intensities of the portlandite (except sample with ECD additive) and unhydrated C_3S peaks than the pure cement sample. Moreover, a trend is clearly visible in these curves: a higher amount of the additive in the samples leads to a lower intensity of the peaks.

The outcome of simultaneous thermal analysis is presented in Figures 6–8. Three endothermic peaks are visible in the DSC analysis graphs of all samples after 28 days of aging (Figure 6). The first peak at a temperature of 90–220 °C concerns the dehydration of many cement hydrates (CSH, ettringite, calcium aluminate hydrate and hydrogarnets), the second peak at a temperature of ~450 °C identifies the decomposition of portlandite, and, at a temperature of 650–750 °C, calcite (which was formed during carbonization of the samples) decomposes [24,29]. The curves of all samples are fairly similar, but a difference is visible in the peak profile between 90 °C and 220 °C. The shoulder at 145 °C is attributed to the dehydration of calcium aluminate hydrates, calcium aluminum silicate hydrates or carboaluminates [29], and it is visible only in the DSC graphs of samples with SCMs. Moreover, in the blank cement sample, the offset point of this peak is reached at a temperature lower than 200 °C, while, in all the samples with additives, the offset point is fixed at a temperature of 220 °C. The shift of the peak towards higher temperatures is also related to the dehydration of the compounds containing the aluminum component because the dehydration of these compounds occurs at ~180–280 °C, i.e., at a higher temperature

than CSH dehydration (110–120 °C) [30,31]. Thus, the DSC analysis results confirm the presence of aluminate-containing phases in the samples with ECD and RECD additives.

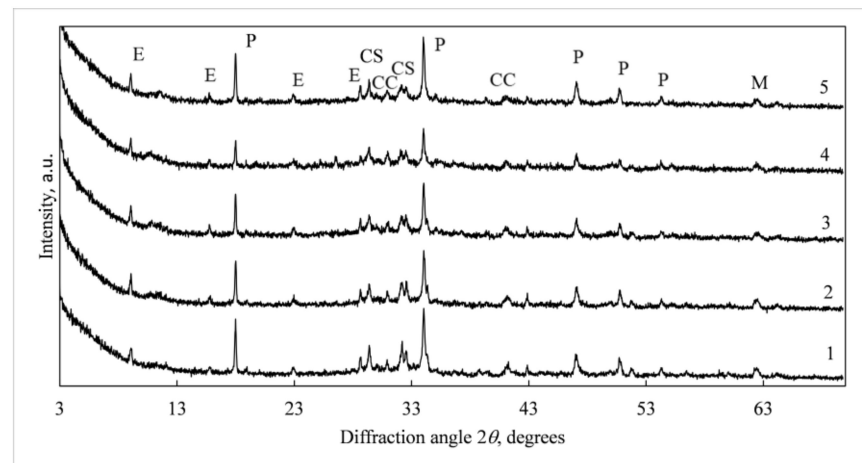


Figure 5. XRD analysis results of samples after 28 days of hydration. 1—OPC (0 wt.%), 2—OPC + 10 wt.% RECD, 3—OPC + 20 wt.% RECD, 4—OPC + 30 wt.% RECD, 5—OPC + 20 wt.% ECD. Indexes: E, ettringite ($\text{Ca}_6(\text{Al}(\text{OH})_6)_2(\text{SO}_4)_3 \cdot 26\text{H}_2\text{O}$); P, portlandite ($\text{Ca}(\text{OH})_2$); CC, calcite (CaCO_3); CS, calcium silicates (C_3S , C_2S); M, periclase (MgO).

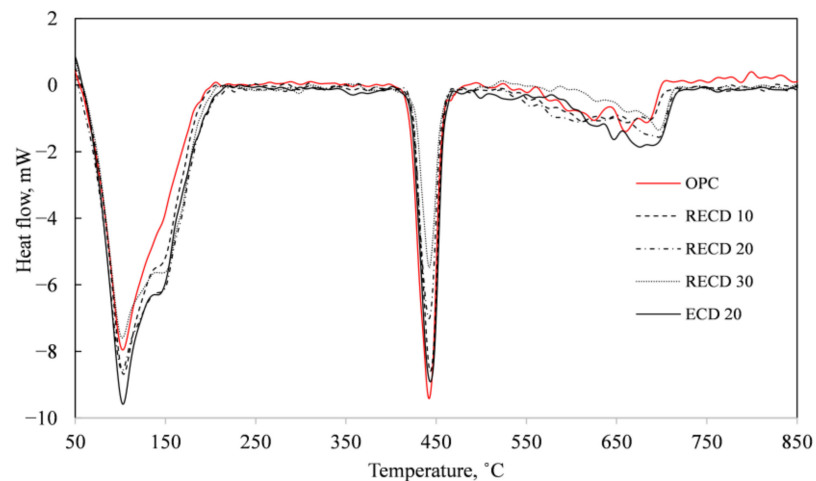


Figure 6. DSC analysis curves of specimens after 28 days of curing.

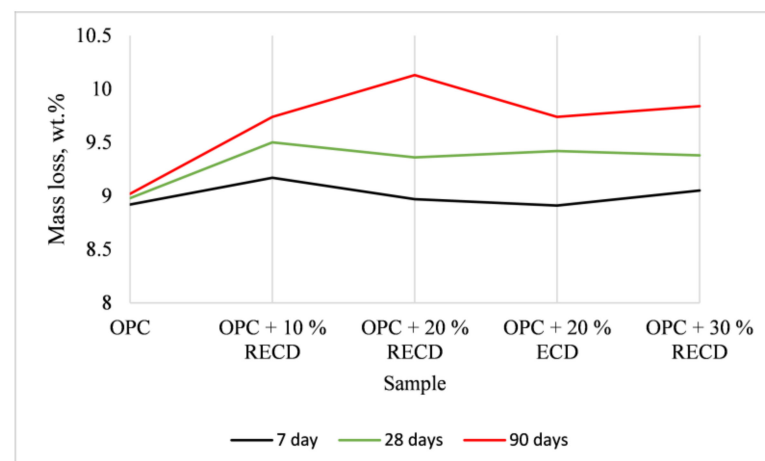


Figure 7. Mass loss of samples in the temperature range of 90–220 °C at various times of hydration.

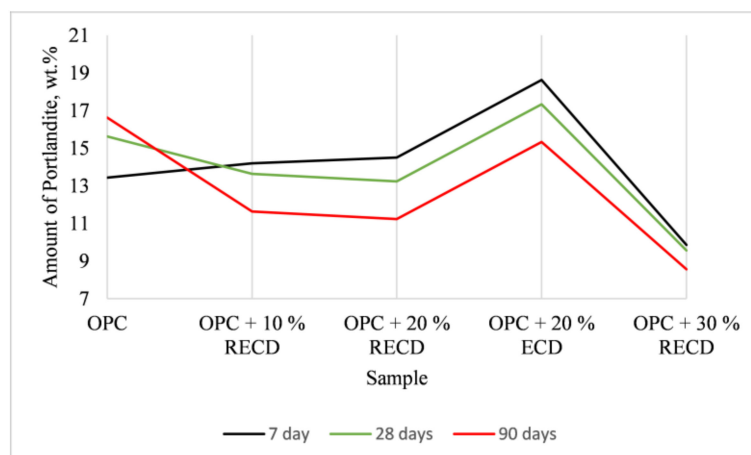


Figure 8. Amount of portlandite in the cement paste at various times of hydration.

Figure 7 shows the mass loss of the samples in the temperature range of 90–220 °C during the dehydration of many cement hydrates, as determined by the thermogravimetric method. The calculated mass ratio of portlandite in the cement paste is presented in Figure 8.

After 7 days of hydration, the mass loss of all samples with additives (except for the sample with 30 wt.% RECD) within the temperature range of 90–220 °C is higher than that of the blank cement specimen (Figure 7). As the duration of hardening increases to 28 and 90 days, this difference becomes even more pronounced. The highest mass losses are observed in the sample with 10 wt.% of RECD. These data show that, in all the samples with additives, more main cement hydrates (CSH, ettringite, calcium aluminate hydrate and hydrogarnets) are formed, which determines the strength of hardened cement. On the other hand, a highly unusual trend can be seen in the curves of the amount of portlandite formed during hydration (Figure 8). After 7 days of hardening, samples with both (RECD and ECD) additives, except for the sample with 30 wt.% RECD—where significantly less cement reacts—showed a higher amount of portlandite than the cement sample. The highest amount of portlandite was found in the sample with nonactivated dust. As pozzolanic activity results have shown that RECD is denoted by high activity, while ECD demonstrates medium-level activity, the higher amount of the formed portlandite can be clarified by the fact that the tested additives have a double effect on cement hydration. The amorphous part of these additives can participate in the pozzolanic reaction, while the crystalline compounds act as crystallization centers and accelerate the hydration process of calcium silicates, during which significantly more portlandite is formed. The less active additive (ECD) reacts more slowly with portlandite; therefore, these samples show a higher amount of portlandite than RECD samples. The progress of the pozzolanic reaction is confirmed by changes in the amount of portlandite as the duration of hardening increases from 7 to 28 and to 90 days. In the blank Portland cement samples, the content of portlandite increases, while, in all the samples with additives, a consistent decrease in the amount of portlandite can be seen with the increasing time of hydration. It should be noted that, even after 28 days of hardening, a higher amount of portlandite is identified in the sample with the ECD additive than in the pure cement sample. Summarizing the results of this part of the research, it can be stated that both nonactivated and activated expanded clay production waste has a double effect on cement hydration—that is, the pozzolanic reaction and the accelerated hydration of calcium silicates occur simultaneously.

The compressive strength outcome (Figure 9) shows that, after 4 weeks of hydration, only the samples with 30 wt.% RECD and 20 wt.% ECD additive are distinguished, with a lower compressive strength compared to the cement sample. The specimens with 10 and 15 wt.% RECD additives (50.9 and 48.5 MPa, respectively) reached the highest compressive strength, whereas the compressive strength values of samples with 20–25 wt.% of RECD

additive (46.7 and 43.3 MPa, respectively) are also higher than the blank cement sample. The samples with 30 wt.% of RECD (41.1 MPa) and 20 wt.% ECD (39.5 MPa) do not pertain to the same strength class (42.5) of cement.

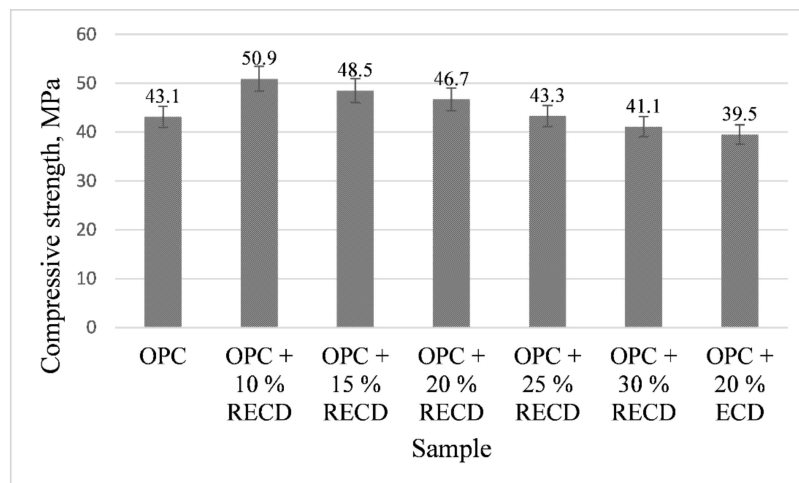


Figure 9. Compressive strength of samples after 28 days of hydration.

Summarizing on the research results of this part, it can be stated that expanded clay kiln dust is a suitable additive for Portland cement. This waste can be used without additional treatment (replacing a smaller amount of Portland cement) or with additional thermal activation. Additional thermal activation is particularly effective if a clay containing a larger amount of kaolinite is used for the production of expanded clay or when kaolinite is used additionally as a flouring material to prevent the aggregate of expanded clay granules from sticking together during combustion.

As already mentioned, expanded clay is manufactured in very large quantities. Using waste from this production in the cement industry offers the potential to replace up to 25 wt.% of cement with this waste material, simultaneously cutting down CO₂ emissions by an equivalent amount. Moreover, this approach would diminish the quantity of waste currently disposed of in landfills and enhance the overall sustainability of cement production.

4. Conclusions

The purpose of this study was to investigate the possibility of applying as supplementary cementitious material a still unexplored industrial material—the waste generated during the production of expanded clay. Evaluations are made of physical and mechanical characteristics of Portland cement with this waste as well as composition of cement hydrates, formed during hydration and hardening processes. The test results of this new material have led to the following conclusions:

- The dust collected in e-filters during the expanded clay calcining process consists of clay minerals (kaolinite, illite and muscovite), impurities (anorthite, calcite, anatase, quartz, magnesite and olivine) and amorphous compounds. The mean diameter of the particles of this dust is 19.99 μm, and its pozzolanic activity reaches 626 mg CaO/g.
- The additional thermal activation at 600 °C temperature increases the pozzolanic activity and the amount of amorphous phases of the tested waste.
- Both additives—thermally activated and nonactivated—accelerate the hydration of cement, especially the hydration reactions of the aluminate-bearing phase, and have a double effect on cement hydration—specifically, the pozzolanic reaction and the accelerated hydration of calcium silicates occur simultaneously.
- The addition of up to 25 wt.% of activated expanded clay kiln dust waste leads to a higher compressive strength of the samples of Portland cement.

Author Contributions: Conceptualization, R.K. and B.S.; methodology, R.K. and B.S.; validation, R.K. and B.S.; investigation, R.K. and B.S.; writing—original draft preparation, R.K. and B.S.; writing—review and editing, R.K.; visualization, B.S.; supervision, R.K. All authors have read and agreed to the published version of the manuscript.

Funding: This research received no external funding.

Institutional Review Board Statement: Not applicable.

Informed Consent Statement: Not applicable.

Data Availability Statement: The data presented in this study are available on request from the corresponding author.

Conflicts of Interest: The authors declare no conflict of interest.

References

- Favier, A.; De Wolf, C.; Scrivener, K.; Habert, G.A. *Sustainable Future for the European Cement and Concrete Industry: Technology Assessment for Full Decarbonisation of the Industry by 2050*; ETH Zurich: Zurich, Switzerland, 2018. [CrossRef]
- Snellings, R.; Mertens, G.; Elsen, J. Supplementary Cementitious Materials. *Rev. Mineral. Geochem.* **2012**, *74*, 211–278. [CrossRef]
- Scrivener, K.; Gartner, E. Eco-efficient cements: Potential economically viable solutions for a low-CO₂ cement-based materials industry. *Cem. Concr. Res.* **2018**, *114*, 2–26. [CrossRef]
- Mehta, A.; Ashish, D.K. Silica fume and waste glass in cement concrete production: A review. *J. Build. Eng.* **2020**, *29*, 100888. [CrossRef]
- Habeeb, G.A.; Mahmud, H.B. Study on properties of rice husk ash and its use as cement replacement material. *Mater. Res.* **2010**, *13*, 185–190. [CrossRef]
- Malaiskiene, J.; Costa, C.; Baneviciene, V.; Antonovic, V.; Vaiciene, M. The effect of nano SiO₂ and spent fluid catalytic cracking catalyst on cement hydration and physical mechanical properties. *Constr. Build. Mater.* **2021**, *299*, 124281. [CrossRef]
- Baiee, A. Development of ultra-high strength cementitious characteristics using supplementary cementitious materials. *J. Eng. Sci.* **2021**, *28*, 111–115. [CrossRef]
- Sullivan, M.S.; Chorzepa, M.G.; Durham, S.A. Characterizing the Performance of Ternary Concrete Mixtures Involving Slag and Metakaolin. *Infrastructures* **2020**, *5*, 14. [CrossRef]
- Agrawal, V.M.; Savoika, P.P. Optimization of binary and ternary concrete composed of fly ash and ultra-fine slag using GRA. *Adv. Concr. Constr.* **2021**, *12*, 283–294. [CrossRef]
- Global Lightweight Aggregates Market Growth 2022–2028. Available online: <https://www.marketandresearch.biz/report/226684/global-lightweight-aggregates-market-growth-2022-2028> (accessed on 1 March 2022).
- Ardakani, A.; Yazdani, M. The relation between particle density and static elastic moduli of lightweight expanded clay aggregates. *Appl. Clay Sci.* **2014**, *93–94*, 28–34. [CrossRef]
- Mlih, R.; Bydalek, F.; Klumpp, E.; Yaghi, N.; Bol, R.; Wenk, J. Light-expanded clay aggregate (LECA) as a substrate in constructed wetlands—A review. *Ecol. Eng.* **2020**, *148*, 105783. [CrossRef]
- Svergzova, S.V.; Sapronova, Z.A.; Starostina, Y.L.; Belovodskiy, E.A. The use of expanded clay dust in paint manufacturing. *IOP Conf. Ser. Earth Environ. Sci.* **2018**, *107*, 012078. [CrossRef]
- Khlystov, A.; Isaev, D.; Suldin, V. Claydite dust—A unique technogenic raw material for heat-resistant concretes production. *IOP Conf. Ser. Mater. Sci. Eng.* **2021**, *1015*, 012070. [CrossRef]
- Fernandez, R.; Martirena, F.; Scrivener, K.L. The origin of the pozzolanic activity of calcined clay minerals: A comparison between kaolinite, illite and montmorillonite. *Cem. Concr. Res.* **2011**, *41*, 113–122. [CrossRef]
- Dinakar, P.; Sahoo, P.K.; Sriram, G. Effect of metakaolin content on the properties of high strength concrete. *Int. J. Concr. Struct. Mater.* **2013**, *7*, 215–223. [CrossRef]
- Tironi, A.; Trezza, M.A.; Scian, A.N.; Irassar, E.F. Kaolinitic calcined clays: Factors affecting its performance as pozzolans. *Constr. Build. Mater.* **2012**, *28*, 276–281. [CrossRef]
- Chi, M.; Huang, R. Effect of montmorillonite as additive on the properties of cement-based composites. *Sci. Eng. Compos. Mater.* **2011**, *19*, 45–54. [CrossRef]
- Ptáček, P.; Frajkorová, F.; Šoukal, F.; Opravil, T. Kinetics and mechanism of three stages of thermal transformation of kaolinite to metakaolinite. *Powder Technol.* **2014**, *264*, 439–445. [CrossRef]
- Gineika, A.; Siauciusas, R.; Baltakys, K. Synthesis of wollastonite from AlF₃-rich silica gel and its hardening in the CO₂ atmosphere. *Sci. Rep.* **2019**, *9*, 18063. [CrossRef]
- EN 196-3:2016; Methods of Testing Cement. Determination of setting Times and Soundness. European Standard: Brussels, Belgium, 2016.
- EN 196-1:2016; Methods of Testing Cement. Determination of Strength. European Standard: Brussels, Belgium, 2016.
- NF P18-513:2012; Metakaolin. Pozzolanic Addition for Concrete. Definitions, Specifications and Conformity Criteria. Association Française de Normalisation: La Plaine Saint-Denis, France, 2012.

24. Zhang, T.; Sun, Z.; Yang, H.; Yanliang, J.; Yan, Z. Enhancement of triisopropanolamine on the compressive strength development of cement paste incorporated with high content of wasted clay brick powder and its working mechanism. *Constr. Build. Mater.* **2021**, *302*, 124052. [[CrossRef](#)]
25. Zhang, B.; Tan, H.; Shen, W.; Xu, G.; Ma, B.; Ji, X. Nano-silica and silica fume modified cement mortar used as Surface Protection Material to enhance the impermeability. *Cem. Concr. Compos.* **2018**, *92*, 7–17. [[CrossRef](#)]
26. Quarcioni, Y.; Chotoli, V.A.F.F.; Coelho, A.C.V.; Cincotto, M.A. Indirect and direct Chapelle's methods for the determination of lime consumption in pozzolanic materials. *Rev. IBRACON Estrut. Mater.* **2015**, *8*, 1–7. [[CrossRef](#)]
27. Luzu, B.; Trauchessec, R.; Lecomte, A. Packing density of limestone calcined clay binder. *Powder Technol.* **2022**, *408*, 117702. [[CrossRef](#)]
28. Babako, M.; Apeh, J.A. Setting time and standard consistency of Portland cement binders blended with rice husk ash, calcium carbide and metakaolin admixtures. *IOP Conf. Ser. Mater. Sci. Eng.* **2020**, *805*, 012031. [[CrossRef](#)]
29. El-Diadamony, H.; Amer, A.A.; Sokkary, T.M.; El-Hoseny, S. Hydration and characteristics of metakaolin pozzolanic cement pastes. *HBRC J.* **2018**, *14*, 150–158. [[CrossRef](#)]
30. Das, S.K.; Mitra, A.; Das Poddar, P.K. Thermal analysis of hydrated calcium aluminates. *J. Therm. Anal. Calorim.* **1996**, *47*, 765–774. [[CrossRef](#)]
31. Rojas, M.F.; Cabrera, J. The effect of temperature on the hydration rate and stability of the hydration phases of metakaolin–lime–water systems. *Cem. Concr. Res.* **2002**, *32*, 133–138. [[CrossRef](#)]

Disclaimer/Publisher's Note: The statements, opinions and data contained in all publications are solely those of the individual author(s) and contributor(s) and not of MDPI and/or the editor(s). MDPI and/or the editor(s) disclaim responsibility for any injury to people or property resulting from any ideas, methods, instructions or products referred to in the content.